ELSEVIER

Engineering Geology 48 (1997) 161–183

ENGINEERING GEOLOGY

Fractal models for predicting soil hydraulic properties: a review

D. Giménez [a,*], E. Perfect [b], W.J. Rawls [a], Ya. Pachepsky [c]

[a] *USDA–ARS, Hydrology Laboratory, Building 007, Room 104, BARC-West, Beltsville, MD 20705, USA*
[b] *Department of Agronomy, University of Kentucky, Lexington, KY 40546-0091, USA*
[c] *USDA–ARS, Remote Sensing and Modeling Laboratory and Department of Botany, Duke University, Durham, NC 27708, USA*

Abstract

Modern hydrological models require information on hydraulic conductivity and soil-water retention characteristics. The high cost and large spatial variability of measurements makes the prediction of these properties a viable alternative. Fractal models describe hierarchical systems and are suitable to model soil structure and soil hydraulic properties. Deterministic fractals are often used to model porous media in which scaling of mass, pore space, pore surface and the size-distribution of fragments are all characterized by a single fractal dimension. Experimental evidence shows fractal scaling of these properties between upper and lower limits of scale, but typically there is no coincidence in the values of the fractal dimensions characterizing different properties. This poses a problem in the evaluation of the contrasting approaches used to model soil-water retention and hydraulic conductivity. Fractal models of the soil-water retention curve that use a single fractal dimension often deviate from measurements at saturation and at dryness. More accurate models should consider scaling domains each characterized by a fractal dimension with different morphological interpretations. Models of unsaturated hydraulic conductivity incorporate fractal dimensions characterizing scaling of different properties including parameters representing connectivity. Further research is needed to clarify the morphological properties influencing the different scaling domains in the soil-water retention curve and unsaturated hydraulic conductivity. Methods to functionally characterize a porous medium using fractal approaches are likely to improve the predictability of soil hydraulic properties. © 1997 Elsevier Science B.V.

Keywords: Water retention; Hydraulic conductivity; Pore surface roughness; Pore volume; Fragmentation

1. Introduction

Predictions of flow and transport processes at a field-scale are needed in a range of applications from petroleum engineering to groundwater pollution assessment. Modern hydrological models require information on transport coefficients and soil-water retention characteristics. A transport coefficient relates a flux to a driving force, whereas a soil-water retention characteristic defines the relationship between water content, θ and pressure potential, ψ. Both properties are closely related to the geometry of a porous medium (i.e. characterizing the distribution of pore, solid space and/or the solid–pore interface). Measurements of hydraulic properties are expensive, time consuming and highly variable (Dirksen, 1991). Prediction of these properties is a viable alternative, especially when the prediction model contains a few parameters sensitive to textural and structural conditions.

* Corresponding author.

PII S0013-7952(97)00038-0

Soils, and to a lesser extent rocks, are heterogeneous systems composed of numerous, different and interacting components (van Damme, 1995). The complex nature of these porous media complicates any prediction of their hydraulic properties.

The classical approach to model a natural porous medium is to assume that a system is invariant by translation. In other words, the system looks the same at different locations and the randomness associated with it can be handled by a finite sample size or by statistical techniques. Fractal systems, on the other hand, are invariant by dilation, i.e. the system looks identical under different magnifications (Adler, 1992). A fractal object has a hierarchical structure with larger units containing smaller units and smaller units enclosing even smaller units and so on ad infinitum. This is known as fractal scaling and is characterized with a power-law distribution. A power-law relating a property of a fractal system to the scale remains the same as the scale changes.

Soil structure is hierarchical with organizational levels ranging from a microscale (tactoides and microaggregates) to a macroscale (clods, pedons) (Hadas, 1987; Dexter, 1988). Scaling of soil physical properties, compatible with a fractal model of soil structure, has been reported previously (Brooks and Corey, 1964; Campbell, 1974; Utomo and Dexter, 1981). A connection between geometry and transport is facilitated when geometry can be described by a small set of parameters such as with a fractal model. Classical semi-empirical power laws such as Archie's law and the Kozeny–Carman equation can be derived by assuming fractal scaling of various physical properties of a porous medium (Muller and McCauley, 1992).

Hardy and Beier (1994), Korvin (1992a), Turcotte (1992) and Feder (1988) have reviewed fractal applications in the earth and geological sciences. Adler (1992) reviewed the application of fractals to quantify transport processes in porous media. Perfect and Kay (1995a) and Senesi (1996) reviewed fractal applications pertaining to soil and tillage research and to soil biology and biochemistry, respectively. The objective of this paper is to review fractal models applied to the prediction of two important soil hydraulic properties, i.e. hydraulic conductivity and the soil-water retention characteristic. The working assumption in all these models is that there exists a theoretical relationship between the geometry of a porous medium and the flow through it.

2. Fractal scaling: basic concepts and evidence for soils and rocks

Mathematical fractals have been used to model the geometry of porous media. The most simple fractals are self-similar fractals constructed by repeating a pattern or generator onto a starting object or initiator. The initiator determines the dimensionality, whereas the generator defines the overall symmetry of the object and produces features at different length scales. The generator pattern is repeated n times and can result in either accretion or reduction of the initiator. The final fractal object contains a range of lengths, $r=1/b^i$, where b is a scaling factor and $i=1, 2, 3\cdots n$. Examples of fractal objects generated by this process are shown in Fig. 1. In the Cantor bar [Fig. 1(a)], the initiator is a solid line and the generator is a broken line. The initial solid line is divided into three equal segments and the middle third is removed (reductive algorithm). The process is then repeated for each of the remaining solid segments. The initiator for the Koch curve [Fig. 1(b)] is also a solid line that is divided into three segments, but the middle segment is now replaced by two segments of the same length as the outer ones (accretive algorithm). The Sierpinski carpet and its three-dimensional counterpart the Menger sponge [Fig. 1(c–d)] are produced by removal of squares or cubes from the initiator which is a plane or a cube, respectively. For example, in the Menger sponge, a cube of unit length is partitioned into 27 smaller cubes and seven cubes are removed. This processes is then repeated for each of the remaining solid cubes. The aforementioned fractals are deterministic since the same operation is repeated at all scales. Randomness can be introduced in these constructions in different ways to produce statistical fractals.

The fundamental equation applying to all frac-

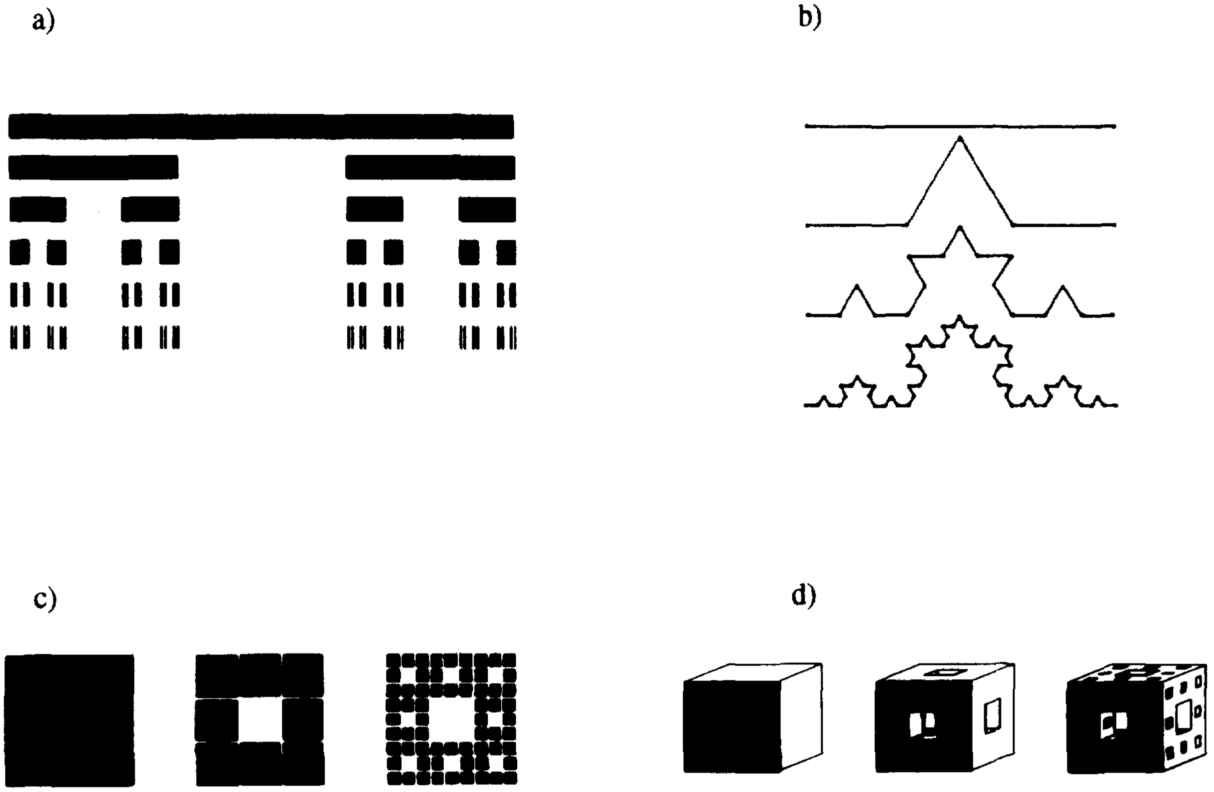

Fig. 1. Examples of deterministic fractals: (a) Cantor bar; (b) Koch curve; (c) Sierpinski carpet; and (d) Menger sponge. Adapted from Perfect and Kay (1995a).

tals is the number–size relationship (Mandelbrot, 1983; Feder, 1988):

$$N(r)=\kappa r^{-D}, \tag{1}$$

where $N(r)$ is the number of elements of length equal to r, κ is the number of initiators of unit length and D is the fractal dimension. Eq. (1) is sometimes used in its cumulative form by replacing $N(r)$ by the number of cumulative elements of length greater than or equal to r, $N(>r)$. A definition of D follows from Eq. (1):

$$D=[\log N(r)-\log \kappa]/\log(1/r) \tag{2a}$$

or

$$D=\log[N(1/b^{i+1})/N(1/b^{i})]/\log(b). \tag{2b}$$

Fractal dimensions can be easily obtained from the models shown in Fig. 1 assuming $\kappa=1$. For the Cantor bar, $N(1/b^{i+1})/N(1/b^{i})=2$, $b=3$ and $D\sim 0.63$; for the Koch curve $N(1/b^{i+1})/N(1/b^{i})=4$, $b=3$ and $D\sim 1.26$; and for the Menger sponge, $N(1/b^{i+1})/N(1/b^{i})=20$, $b=3$ and $D\sim 2.73$.

Fractal dimensions in natural objects are obtained from measurements. The basic measurement technique consists of measuring a property with units of regular shape and different characteristic size, ℓ. If the scaling of the property is fractal, the number of units of a certain characteristic size, $N(\ell)$, is related to ℓ according to Eq. (1):

$$N(\ell)\propto \ell^{-D}. \tag{3a}$$

The scaling of the property measured (length, area, or volume) is obtained from Eq. (3a) as:

$$N(\ell)\ell^{D_T}\propto \ell^{D_T-D}, \tag{3b}$$

where D_T is the topological dimension of the measuring units: $D_T=1$, 2 and 3 for a line, plane and volume, respectively.

Several different fractal dimensions can be used to characterize the geometry of a porous medium in relation to transport processes. Fractal scaling of aggregated mass, pore volume, pore surface (Fig. 2), and size-distribution of fragments have all been observed for geological materials such as rocks and soils.

2.1. Fractal dimension of mass

A fractal dimension of mass, D_m, quantifies space-filling characteristics of the solid in a space of radius r (Fig. 2). For a mass fractal, scaling of mass, M, follows a relationship of the form:

$$M \propto r^{D_m},\ D_m \leq d, \tag{4}$$

where d is the embedding dimension, defined as the minimum number of coordinates needed to enclose an object, i.e. $d=2$ and 3 correspond to a two- and a three-dimensional space, respectively. Eq. (4) can also be applied to separate entities (e.g. soil aggregates) of different radii but similar shape. A fractal scaling of mass implies a decrease in bulk density, ρ, with r:

$$\rho_i/\rho_1 = (r_i/r_1)^{D_m - d}, \tag{5}$$

where ρ_i and ρ_1 are bulk densities measured over a radius r_i and r_1, respectively, with $r_i > r_1$. In a system of small aggregates (units) clustering into larger ones, aggregate density scales as $\rho_{i+1} = p\rho_i$, with $0<p<1$. The size of an aggregate scales as $r_{i+1} = br_i$ for $b>1$, with $i=1, 2, 3 \cdots n$. At the nth generation, $\rho_n = p^n\rho_1$ and $r_n = b^n r_1$. Combining these two equations and eliminating n:

$$\rho_n/\rho_1 = (r_n/r_1)^{\log p/\log b}. \tag{6}$$

Comparing Eqs. (5) and (6), it can be seen that $D_m = d + (\log p/\log b)$. Since ($\log p/\log b$) is negative $D_m \leq d$ (Onoda and Toner, 1986) and the density of a fractal object decreases with increasing values of r. For the Menger sponge $d=3$, $p=20/27$ and $b=3$ and, therefore, $D_m \sim 2.73$, which is the same D obtained from Eq. (1).

Fractal dimensions of mass have been measured using several techniques. Images of soil or rock sections are covered with square grids each with a different square size ℓ and the total number of squares in contact with the solid space, $N(\ell)$, is obtained for each square size (box-counting technique). The value of D_m is calculated from a plot of the number of squares counted vs size, according to Eq. (3a). Others have obtained D_m from measurements of mass or bulk density on aggregates of different sizes [Eqs. (4) and (5), respectively]. Table 1 summarizes D_m values found in the literature on soils. Typically, values for D_m are between 2.75 and 2.99 without any apparent trend with soil texture (Table 1). This lack of sensitivity suggests that other constants in Eqs. (1), (4) and (5) may be more useful for characterizing the geometry of porous media for the purpose of predicting transport processes. The constants in Eqs. (4) and (5) are related to the lacunarity or uniformity in the distribution of mass within a fractal object (Gouyet, 1996). Zeng et al. (1996) showed that lacunarity, measured from spatial variation of bulk density, was an important discriminator of soil structure.

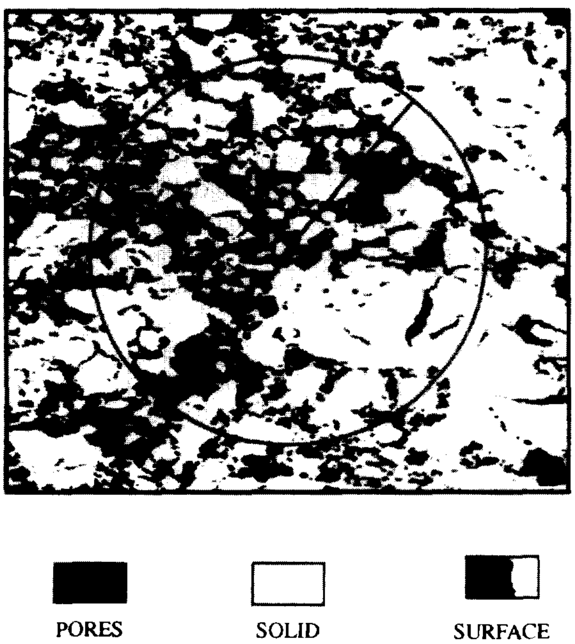

Fig. 2. Cross-section of a porous medium showing distribution of solid, pore space and pore surface in an area of radius r.

Table 1
Summary of values of fractal dimension of mass, D_m, found in the literature

Soil/soil texture	D_m[a]	Range	Method	Reference
Sand	2.95	10^{-2}–10^6 μm	Eq. (3a)	Bartoli et al. (1991)
Sandy loam-1	2.75	1–10 mm	Eq. (4)	Young and Crawford (1991a)
Sandy loam-2	2.93	1–10 mm	Eq. (4)	Young and Crawford (1991a)
Fine sandy loam	2.88	0.06–2.1 mm	Eq. (4)	Anderson and McBratney (1995); Rieu and Sposito (1991b)[b]
Sandy loam/loam	2.92	0.75–6.5 mm	Eq. (5)	This study[c]
Loam	2.95	0.75–6.5 mm	Eq. (5)	This study[c]
Loam	2.85	0.25–7.5 cm	Eq. (5)	Giménez et al. (1994)[d]
Silt loam	2.93	0.75–6.5 mm	Eq. (5)	This study[c]
Silt loam	2.90	0.06–2.1 mm	Eq. (5)	Anderson and McBratney (1995); Rieu and Sposito (1991b)[b]
Silt loam	2.95	0.75–6.5 mm	Eq. (5)	This study[c]
Silt loam	2.97	0.75–6.5 mm	Eq. (5)	This study[c]
Silty	2.92	10^{-2}–10^6 μm	Eq. (3a)	Bartoli et al. (1991)
Clay loam	2.93	0.75–6.5 mm	Eq. (5)	This study[c]
Clay loams	1.95–1.98	NA[d]	Eq. (3a)	Crawford and Matsui (1996)
Silty clay loams	1.93–1.98	NA[d]	Eq. (3a)	Crawford and Matsui (1996)
Clay	2.96	0.06–2.1 mm	Eq. (5)	Anderson and McBratney (1995); Rieu and Sposito (1991b)[b]
Clay	1.98	NA[d]	Eq. (3a)	Crawford and Matsui (1996)
Clay	2.88	0.25–7.5 cm	Eq. (5)	Giménez et al. (1994)[e]
Clay	2.89	0.25–7.5 cm	Eq. (5)	Giménez et al. (1994)[e]
Sharpsburg soil	2.95	0.11–7.00 mm	Eq. (5)	Rieu and Sposito (1991b)[f]
Sharpsburg soil	2.89–2.90	0.08–3.19 mm	Eq. (5)	Anderson and McBratney (1995)[g]

[a]Values of D_m in the ranges 1–2 and 2–3 correspond to embedding dimensions of two and three, respectively.
[b]Data from Chepil (1950).
[c]Data from Lin (1971).
[d]NA: not available.
[e]Data from Larson and Padilla (1990).
[f]Data from Wittmus and Mazurak (1958).
[g]Data from Eghball et al. (1993).

2.2. Fractal dimension of pore volume

A fractal dimension of pore volume, D_v, quantifies the space-filling properties of pore volume, V_p, in a space of radius r (Fig. 2). Scaling of pore volume follows a power-law of the form:

$$V_p \propto r^{D_v},\ D_v \leq d, \tag{7}$$

where D_v is the fractal dimension of pore volume. Fig. 2 shows that the space within the circle with radius r is composed by mass and pore space. Thus, Eqs. (4) and (7) are similar in form, but represent scaling of complementary properties, i.e. mass and pore space. The equivalent of Eq. (5) is the scaling of porosity ϕ, which measures the density of pore space. Table 2 summarizes published D_v values for rocks and soils. Scaling of pore volume has been studied using two-dimensional images of cross-sections of soils and rocks with either the box-counting technique [Eq. (3a)] or by a pore-size count [Eq. (1)]. A comparison between Tables 1 and 2 shows that D_v values are generally smaller and span a larger range than D_m values.

2.3. Fractal dimension of pore surface

A fractal pore surface area, S, scales with r according to (Fig. 2):

$$S \propto r^{D_s},\ D_T \leq D_s \leq d, \tag{8}$$

where D_s is a fractal dimension of pore surface area. Several techniques have been used to measure D_s. A surface can be probed with molecules of different characteristic size ℓ, and the D_s obtained by plotting the amount of adsorbed molecules per

Table 2
Summary of values of fractal dimension of pore volume, D_v, found in the literature

Material	D_v	Range	Reference[a]
Sandstone	1.69	10^{-1}–10^2 μm	Hansen and Skjeltorp (1988)
Sandstone	1.70	<1 mm	Jacquin and Adler (1987)
Chalk	1.80	10 mm	Jacquin and Adler (1987)
Dolomite	1.40	<5mm	Jacquin and Adler (1987)
Loam to silt loam[b]	1.82–1.81	50–250 μm	Anderson et al. (1996)
Loam to silt/clay loam[b]	1.72–1.79	50–250 μm	Anderson et al. (1996)
Silt loam-1[c]	1.44	1–10 mm	Peyton et al. (1994)
Silt loam-2[c]	1.22	1–10 mm	Peyton et al. (1994)
Silty clay loam[b]	1.78–1.70	50–250 μm	Anderson et al. (1996)
Clay loam[b]	1.68–1.75	50–250 μm	Anderson et al. (1996)
Clay–loam-1[d]	1.59	0.5–40 mm	Giménez et al. (1997a)
Clay–loam-2[d]	1.49	0.5–40 mm	Giménez et al. (1997a)
Clay	1.74	10–150 μm	Ozhovan et al. (1993)
Clay[b]	1.79–1.78	50–250 μm	Anderson et al. (1996)
Clay[b]	1.85	50–250 μm	Anderson et al. (1996)

[a]Ozhovan et al. (1993) determined D_v from a pore-size count [Eq. (1)], the rest of the authors used the box-counting technique [Eq. (3a)].
[b]A.N. Allison, personal communication.
[c]Silt loam-1, forest; silt loam-2, grassland.
[d]Clay–loam-1, field cultivated with a chisel plow (fall) and a disc (spring); clay–loam-2, field cultivated only with disc in the spring.

unit mass of adsorbent, n, versus ℓ, according to Eq. (3a). An alternative is to use the same probing molecule but vary the size of the adsorbent, r. The scaling of n with r is (Avnir et al., 1985):

$$n \propto r^{D_s - 3}. \tag{9}$$

Neimark (1992) proposed to estimate D_s directly from Eq. (3b), by defining ℓ as a mean radius of curvature of a set of equicurvature surfaces. Equicurvature surfaces can be obtained from the intrusion of a nonwetting fluid (e.g. mercury) into a porous medium, or from adsorption or desorption isotherms.

Table 3 summarizes published values of D_s for various porous media. Values of D_s are related to mineral composition and soil organic matter content. Larger fractal dimensions are associated with clay minerals (Avnir et al., 1985; van Damme, 1995). Quartz particles, on the other hand, exhibit smoother surfaces that result in fractal dimensions close or equal to two (Avnir et al., 1985; Barak et al., 1996). Bartoli et al. (1992) found that D_s increased linearly with organic matter content for two Oxisols in the range of pore diameters between about 0.1 and 40 μm. They also reported a negative relationship between D_s and pore volume indicating that D_s was a measure of the degree of pore volume filling. A decrease in values of D_s after oxidation of soil organic matter and carbohydrates was observed for pores <1 μm and attributed to a decrease of bonds between particles (Pachepsky et al., 1995a; Pachepsky et al., 1996a). At the same time, D_s values decreased after organic matter oxidation for pores with diameters between about a 1.5 and 5 μm range (Pachepsky et al., 1995a).

Pore outline fractal dimension $D_o = D_s - 1$ has been determined using image analysis of pore outline. The embedding dimension was $d = 2$ in these studies. Pore outline fractal dimensions are sensitive to soil type (Kampichler and Hauser, 1993; Anderson et al., 1996), soil management (Pachepsky et al., 1996b) and soil consolidation after tillage (Giménez et al., 1997a).

There seems to be ample evidence for the fractal nature of pore surfaces of different earth materials with D_s values covering a wide range between 2 and 3 (Table 3), which is larger than the ranges of either D_m or D_v. This suggests that the D_s may be

Table 3
Summary of values of fractal dimension of pore surface, D_s, found in the literature

Material	D_s[a]	Range	Method	Reference
Sandstone	1.69	10^{-1}–10^{2} μm	Eq. (3a)	Hansen and Skjeltorp (1988)
Sandstones	2.57–2.87	10^{-3}–10^{2} μm	Eq. (3a)	Katz and Thompson (1985)
Sandstones	2.49–2.89	10^{-1}–$>10^{1}$ μm	Eq. (3a)	Krohn (1988)
Carbonates	2.27–2.75	10^{-1}–$>10^{0}$ μm	Eq. (3a)	Krohn (1988)
Carbonates	2.01–2.97	10^{1}–10^{3} μm	Eq. (9)	Avnir et al. (1985)
Shales	2.54–2.75	10^{-1}–$>10^{0}$ μm	Eq. (3a)	Krohn (1988)
Sandy	2.75	10^{-2}–10^{2} μm	Eq. (13)	Bartoli et al. (1991)
Sandy loams	2.28–2.32	10^{-1}–10^{3} μm	Eq. (9)	Sokolowska (1989)
Sandy loam	2.37	10^{-3}–10^{2} μm	Eq. (9)	Borkovec et al. (1993)
Loams	2.31–2.40	10^{-1}–10^{3} μm	Eq. (9)	Sokolowska (1989)
Loam	2.40	10^{-3}–10^{2} μm	Eq. (9)	Borkovec et al. (1993)
Loam-1	2.23–2.28	10^{-2}–1 μm	Eq. (13)	Pachepsky et al. (1996a)
Loam/silt loam[b]	1.20–1.25	50–250 μm	E/D[c]	Anderson et al. (1996)
Loam–silt/clay loam[b]	1.20–1.22	50–250 μm	E/D[c]	Anderson et al. (1996)
Silty	2.69–2.90	10^{-2}–10^{2} μm	Eq. (13)	Bartoli et al. (1991)
Silt[d] loam-1	1.10	[e]NA	Eq. (3a)	Young and Crawford (1991b)
Silt[d] loam-2	1.31	[e]NA	Eq. (3a)	Young and Crawford (1991b)
Silty clay loam[b]	1.23	50–250 μm	E/D[c]	Anderson et al. (1996)
Silty clay	2.38	10^{-3}–10^{2} μm	Eq. (9)	Borkovec et al. (1993)
Clay loam	2.44	10^{-3}–10^{2} μm	Eq. (9)	Borkovec et al. (1993)
Clay loam[b]	1.17–1.18	50–250 μm	E/D[c]	Anderson et al. (1996)
Clays-1[f]	2.49–2.62	10^{-2}–10^{2} μm	Eq. (9)	Bartoli et al. (1992)
Clays-2[f]	2.86–2.90	10^{-1}–10^{1} μm	Eq. (9)	Bartoli et al. (1992)
Clay–loam-1[g]	1.25	0.5–40 mm	Eq. (9)	Giménez et al. (1997a)
Clay–loam-2[g]	1.22	0.5–40 mm	Eq. (9)	Giménez et al. (1997a)
Clay[b]	1.15–1.24	50–250 μm	E/D[c]	Anderson et al. (1996)
Clay[b]	1.16–1.19	50–250 μm	E/D[c]	Anderson et al. (1996)

[a]Values of D_s in the ranges 1–2 and 2–3 correspond to embedding dimensions of two and three, respectively.
[b]A.N. Allison, personal communication.
[c]Erosion–dilation method on images of soil section.
[d]Silt loam-1, arable land; silt loam-2, meadow.
[e]NA: not available.
[f]Clays-1, rich in gibbsite; clay-2, rich in goethite.
[g]Clay–loam-1, field cultivated with a chisel plow (fall) and a disc (spring); clay–loam-2, field cultivated only with disc in the spring.

more useful than either D_m or D_v for characterizing soil structure in models to predict transport processes.

2.4. Fractal dimension of fragmentation

Fragmentation is a widespread phenomenon in nature. Tillage and weathering are examples of processes leading to soil fragmentation. A scale-invariant fragmentation process leads to a distribution of fragment sizes that follow the cumulative form of Eq. (1), with D being the fragmentation fractal dimension, D_f. Estimates of D_f range between 1 and 5 (Wu et al., 1993). According to the fragmentation model of Turcotte (1986, 1992), which assumes an incomplete fragmentation with a scale-invariant probability of fragmentation, D_f should have values between 0 and 3. Physical interpretations of $D>3$ in Eq. (1) are not straightforward (Crawford et al., 1993b; McBratney, 1993; Perfect et al., 1993).

The most direct way to estimate D_f is to measure the number–size distribution of objects and then fit Eq. (1) to these data. However, it is traditionally the mass–size distribution that is measured in geology and soil science. Tyler and Wheatcraft

(1989) and Perfect and Kay (1991) used Eq. (1) to calculate D_f from the mass–size distribution of particles and aggregates, respectively. Eq. (1) was implemented indirectly by transforming a set of relative mass classes to particle/aggregate number, $N(>r)$. Each mass class comprises particle/aggregate sizes between a lower and an upper size bound. The calculation of particle number from mass implies assumptions about a characteristic particle size (representing the size class) and particle shape and density. The most common assumptions are that particle size is the arithmetic mean between the upper and lower bounds and that particle density and shape are constant (Tyler and Wheatcraft, 1989; Perfect and Kay, 1991; Perfect et al., 1992). Scale-invariant shape and/or bulk density, however, cannot be assumed for soil-aggregates that are themselves considered to be fractal in the scaling of mass and/or voids (Logsdon et al., 1996).

Several improvements to the calculation procedure of D_f have been proposed. Tyler and Wheatcraft (1992a) proposed to calculate D_f from mass–size distribution. The method does not require an estimation of particle size and is more sensitive to deviations from fractal scaling than the method of cumulative number. Based on results with the new method, they argued that only a limited number of soil textural classes can exhibit fractal distribution of particle sizes. Kozak et al. (1996) proposed an algorithm that does not use the arithmetic mean as a characteristic size of a mass class. Both modifications, however, still assume constant particle/aggregate shape and density. Rasiah et al. (1993) presented a method that does not require the assumption of scale-invariant particle density and probability of fragmentation, but still assumes constant shape of soil particles. Despite the theoretical problems to estimate and interpret D_f, this fractal dimension is still potentially useful to model soil hydraulic properties because particle size distribution is one of the soil properties more readily available.

2.5. *Fractal dimensions of connectivity*

An important property for transport through a porous medium is its connectivity. An intrinsic connectivity property of fractal systems is the spreading dimension, d_e, defined as the number of sites, NS, accessible from a given origin in at most N_c steps:

$$NS(N_c) \propto N_c^{d_e}, \tag{10}$$

where N_c is called the chemical distance or distance of connectivity. Jacquin and Adler (1987) determined d_e for a number of rocks. It can be shown (Gouyet, 1996) that $d_e = D/D_{min}$, where D is the mass fractal dimension of a fractal network (for a Menger sponge $D \sim 2.73$) and D_{min} is the fractal dimension of the minimum path length between two points in the network.

Another intrinsic dimension is the spectral dimension, defined as the average number of sites visited by a random walker after N_w steps (Crawford et al., 1993a; Anderson et al., 1996):

$$NS(N_w) \propto N_w^{\bar{d}/2}, \tag{11}$$

where, in the context of diffusion in soil, $\bar{d} = D_v/D_w$ and D_w is the fractal dimension defining a random walk. The spectral dimension is particularly relevant for simulating diffusion in a fractal network. For a particle diffusing in a macroscopically homogeneous medium, its mean square displacement, r^2, is linearly related to time, t. In a fractal medium, $r^2 \propto t\epsilon$, where $\epsilon = \bar{d}/D_w < 1$, which indicates that diffusion is slower than in a macroscopically homogeneous medium (anomalous diffusion). Crawford et al. (1993a) and Anderson et al. (1996) measured $\bar{d}$ and D_v from two-dimensional thin sections of soils. Their data shows that $\bar{d}$ and D_v are correlated and therefore the variability of ϵ among soil structures is less than that of either $\bar{d}$ or D_v. Values of ϵ were between 0.61 and 0.90 for soils. Values of $\bar{d}$ obtained from thin sections could be of limited value because ϵ is also a function of water content, θ. Guerrini and Swartzendruber (1994) and Glasbey (1995) showed that water and gas diffusion, respectively, become more anomalous at lower water contents.

2.6. *Relationships between different fractal dimensions*

The relationship among the different fractal dimensions is important because it could simplify modeling of soil properties in general, and shed some light on the validity of the fractal models used for hydraulic properties in particular. For deterministic fractals such as the Sierpinski carpet or the Menger sponge, Eq. (1) describes the scaling of mass, pores and the solid–pore interface with $D=D_m=D_v=D_s$ (Friesen and Mikula, 1987; Rieu and Sposito, 1991a; Perfect and Kay, 1995b).

For natural fractals, not generated by an exact iterative procedure, it is possible that D_m, D_v and D_s are not equal. Katz and Thompson (1985) proposed that $D_s=D_v$ in sandstones and used measured D_s to calculate porosity. Ghilardi et al. (1993) used a simulation experiment to study the scaling properties of a porous medium formed by the deposition of a collection of granules with size distributions of the type described by Eq. (1). They found that pore space and pore surface roughness of the resulting porous medium showed fractal scaling, with $D_f=D_v=D_s$. In a later paper, Ghilardi and Menduni (1996) showed that the equality among fractal dimensions defining a fragmentation process and those characterizing the spatial distribution of the fragments is a function of porosity and of the value of the exponent in the power-law of particle-size distribution. Crawford et al. (1993b), on the other hand, claimed that experimentally determined number–size relationships do not convey information on scaling of mass or pore volume of the original structure because mechanical disruption randomly breaks the structure destroying information on the spatial arrangement of the constituent particles. According to Crawford et al. (1993b), assuming scale-invariant probabilities of fragmentation, D_f is related to D_s. The particles in the model of Crawford et al. (1993b) are solid, and therefore they are a better representation of rock fragments than they are of soil aggregates. For rock fragments, Nagahama (1993) has shown that D_f and D_s are related and that the values of both fractal dimensions increase with the energy density that is available for fragmentation. The relationship between D_f, D_m and D_s is discussed in detail by Perfect (1997).

There has not been experimental confirmation of the equality $D_m=D_v$ for soils. A comparison between Tables 1 and 2 shows that, in general, D_v exhibits a larger range of values than D_m. Bartoli et al. (1991) found that the sandy and silty soils they studied did not exhibit fractal scaling of pore volume and that $D_m=1.1D_s$, suggesting that their three soils were mass and surface fractals (see Tables 1 and 3). Crawford and Matsui (1996) argued that since pore and solid complement each other in space (Fig. 2), only one of the two can be fractal. They measured D_m and D_v on images of thin sections of nine soils. Fractal dimensions were determined on subsamples of different size, r. They found that only D_m was constant with r and concluded that their samples were mass fractal. However, the thickness of a thin section and its impregnation conditions mean that only a part of the pore system is visible and used for analysis. The nonvisible part is analyzed as solid. This experimental artifact complicates the interpretation of their results, particularly the ones at small r.

In conclusion, there is no clear experimental evidence about the nature of the relationship among the different fractal dimensions characterizing soil structure. This limitation should be considered when analyzing the different approaches to model soil hydraulic properties.

3. Fractal models for soil hydraulic properties

3.1. Soil-water retention

Empirical models of soil-water retention, $\theta(\psi)$, have been known for a long time (Brooks and Corey, 1964; Campbell, 1974; van Genuchten, 1980; Ross et al., 1991). The main problem with empirical formulations is their minimum impact on the understanding of soil-water phenomena, which limits the possibilities of extrapolating results to soils outside the data set that was used to fit the model.

Three types of theoretical models for $\theta(\psi)$ have been proposed based on a fractal organization of soil structure. The first type is a mass fractal (Sierpinski carpet or Menger sponge) in which the fractal dimensions of mass, pore surface and pore volume have the same value (Rieu and Sposito, 1991a; Perfect et al., 1996, 1997). The second approach is based on a fractal surface in which water is retained in cavities and irregularities and connected through thin films (de Gennes, 1985; Pape et al., 1987; Toledo et al., 1990). At higher water contents, a surface fractal also results in a power-law distribution of pore sizes (Friesen and Mikula, 1987). In this approach, there is no consideration of the scaling of mass. The third approach considers a fractal pore size distribution without any assumption about the geometry of mass and the solid-pore interface (Tyler and Wheatcraft, 1990; Pachepsky et al., 1995b; Perrier et al., 1996).

The basic equation used to derive a fractal model of water retention assumes a power-law distribution of pore volumes according to Eq. (1) in its cumulative form, $N(>r)$. The expression relating pore volume, $V_p(>r)$, to pore diameter, r, is given by (Pfeifer and Avnir, 1983; Friesen and Mikula, 1987; Perrier et al., 1996):

$$-V_p(>r) \propto N(>r)r^3 = Ar^{3-D} + V_o, \qquad (12)$$

where A is a constant that reflects both the size and geometry of a porous media sample and V_o is a constant of integration (Pachepsky et al., 1995b; Perrier et al., 1996). Soil-water content, θ, is the amount of water retained in pores $<r$, expressed per unit of total (sample) volume V_T, i.e. $V_p(<r)/V_T$. Porosity, ϕ, is then $\phi = \theta + V_p(>r)/V_T$ and $d\theta/dr = -dV(>r)/dr$. Eq. (12) assumes that the accessibility of any pore does not depend on smaller pores. Commonly, a Young–Laplace equation of the form $r \propto 1/\psi$ is used as a pore desaturation function, where ψ is the pressure necessary to evacuate a pore with diameter $>r$. All pores with a diameter $r_i \leq r$ are saturated with water, while pores with $r_i > r$ are completely empty.

Ahl and Niemeyer (1989) employed Eq. (12) to model a soil-water retention curve, without evaluating the constant of integration V_o. Their equation is written as:

$$\theta \propto \psi^{D-3}. \qquad (13)$$

This expression can be derived for a porous medium with a fractal distribution of mass, fractal distribution of pore volume, or fractal pore surface (Friesen and Mikula, 1987; Crawford et al., 1995; Perrier et al., 1996). This represents a problem if morphologically derived fractal dimensions are to be used in the prediction of retention and/or transport properties in porous media because mass, volume, and surface fractal dimensions usually do not coincide. This model does not contain upper and lower scaling limits. Eq. (13) has been applied to soil-water retention data (Ahl and Niemeyer, 1989) and to mercury porosimetry data (Friesen and Mikula, 1987; Bartoli et al., 1991; Bartoli et al., 1992; Bartoli et al., 1993; Friesen and Laidlaw, 1993; Pachepsky et al., 1995a).

Bird et al. (1996) proposed to complement Eq. (13) with a desaturation function of the form $\theta \propto \psi^{-2}$ to account for water held in surface irregularities for $r_i > r$. Their equation is:

$$\theta \propto B\frac{\psi^{D-3}}{D-1} - B\frac{\psi^{-2}\psi_{min}^{D-3}}{D-1} + \frac{\psi^{D-3}}{3-D} - \frac{\psi_{max}^{D-3}}{3-D}, \qquad (14)$$

where B is a constant <1. Eq. (14) incorporates lower, ψ_{max} and upper, ψ_{min}, limits to the distribution of pressure potentials and it does not predict complete desaturation at pressure potentials lower than ψ_{max} ($r_i > r$). The desaturation function proposed by Bird et al. (1996) corresponds to a nonfractal surface (de Gennes, 1985), and therefore is expected to perform poorly in materials with fractal surfaces such as sandstones (Davis, 1989). To our knowledge, Eq. (14) has not been tested against experimental soil-water retention.

Tyler and Wheatcraft (1990), using a Sierpinski carpet algorithm, derived an expression for soil water retention similar to Eq. (13). Their formula incorporates a saturated water content, θ_s, and an air entry value, ψ_{min}, as an upper limit for a fractal scaling, i.e.:

$$\theta/\theta_s = (\psi/\psi_{min})^{D-2}, \qquad (15)$$

where D is a fractal dimension in the range $0 \leq D \leq 2$ (a consequence of the two-dimensional construction selected to develop the model). Eq. (15) assumes that the lower limit of water content is zero, i.e. $\psi \rightarrow \infty$ and $\theta \rightarrow 0$. Tyler and Wheatcraft (1990) recognized that a Sierpinski carpet yields a porosity, or saturated water content, θ_s, of unity. Since this property of the carpet is not realistic for soils, they developed

Eq. (15) from the cumulative pore number–size distribution of the Sierpinski carpet, which at high enough number of iterations, is a good approximation of Eq. (1). From that point of view, the Tyler and Wheatcraft (1990) model is a representation of the scaling of a fractal pore space without consideration on the distribution of mass.

Equations similar to Eq. (15) were proposed by Brooks and Corey (1964) and Campbell (1974). In the Brooks and Corey (1964) formulation, a residual water content, θ_r, is subtracted from the numerator and denominator of the left hand side of Eq. (15), i.e.:

$$S_e = (\theta - \theta_r)/(\theta_s - \theta_r) = (\psi/\psi_{min})^{-\lambda}, \quad (16)$$

where S_e is an effective saturation, λ is a pore size distribution parameter and θ_r is defined as a water content at $\psi \to \infty$. Rawls et al. (1982) summarized θ_s, θ_r, λ and ψ_{min} for the eleven USDA textural classes using data from 5350 soil horizons. Values of λ were in the range $0.13 \leq \lambda \leq 0.59$ increasing from sand to clay. Brakensiek and Rawls (1992) used the $\lambda = 2 - \lambda$ values in Rawls et al. (1982) to calculate D values according to Eq. (15). Since Rawls et al. (1982) fitted the Brooks and Corey (1964) model [Eq. (16)], the D values in Brakensiek and Rawls (1992) are in the range between saturation and residual water content. Clapp and Hornberger (1978) fitted water retention data from 1446 horizons to Eq. (16) with $\theta_r = 0$. Their λ values were $0.09 \leq \lambda \leq 0.25$, increasing also with clay content. The smaller range of fitted λ values for the Clapp and Hornberger (1978) data set, as compared with those in Brakensiek and Rawls (1992), is probably caused by the choice of $\theta_r = 0$ made by Clapp and Hornberger (1978).

Rieu and Sposito (1991a) developed a model of soil structure for a mass fractal (Menger sponge) in which the scaling of mass, pore volume and pore–solid interface are fractal with the same fractal dimension ($D_m = D_v = D_s$). They developed the concept of incomplete fragmentation to account for the mechanical coherence of structured soils. In their model, self-similar soil aggregates are separated by a self-similar network of fractures. A bulk volume is formed by aggregates of different size with a number–size relationship given by Eq. (1). In the completely-fragmented medium, an aggregate of volume V_i contains a number N of aggregates of a smaller volume class, V_{i+1} and a pore volume P_i formed by pore elements arranged around the volumes V_{i+1}, with $i = 0 \cdots n-1$; V_n corresponds to the residual solid volume. The scaling between successive volumes and/or pores sizes is given by a linear similarity ratio $b < 1$. A pore coefficient, Γ, defined as the quotient P_i/V_i, is related to b by $\Gamma = 1 - b^{3-D}$. The fractal dimension D_f of the porous medium is obtained according to Eqs. (2a) and (2b). In an incompletely fragmented medium, the number of aggregates of volume V_i is less than that in a completely fragmented medium. At each level of the construction, part of the pore space is replaced by bridges linking some of the aggregates and bringing mechanical coherence to the soil mass. The degree of fragmentation is determined by a probability of fragmentation or clustering factor, F ($0 < F < 1$), obtained from $F = 1 - \Gamma_r/\Gamma$, where Γ_r is the pore coefficient for the incompletely fragmented soil. The Rieu and Sposito (1991a) expression for water retention for structured soils is:

$$\theta = \theta_s - 1 + \left[\frac{\psi}{\psi_{min}}\right]^{D_{if}-3}, \quad (17)$$

where D_{if} is a fractal dimension for a partially fragmented (or structured) soil mass and θ_s is the saturated water content. Note that $\theta_s \to 1$ as $\psi \to \infty$, which corresponds to a Menger sponge with an infinite number of recursive steps (Perrier et al., 1996). By defining a residual solid volume V_n, Rieu and Sposito (1991a) set $\psi_{max} < \infty$ to represent both the solid and the pore spaces. Values for D_{if} were between 2.76 (sandy soil) and 2.99 (silty clay) (Rieu and Sposito, 1991b,c) in agreement with published data on fractal dimensions of soil mass (Table 1). The model deviates from experimental data, however, at water contents close to saturation and at very low water contents.

Perrier et al. (1996) evaluated the constant of integration V_o in Eq. (12) as a pore volume between a lower, $r_{min} = 0$, and an upper, r_{max}, pore diameter:

$$V_o = A r_{max}^{3-D}. \quad (18)$$

The V_o is then a representation of maximum possible pore space. The definition of V_o implies that the entire pore system is fractal. Introduction of V_o resulted in a formulation similar to the Rieu and Sposito (1991a) model:

$$\theta=\theta_s+\frac{V_o}{V_T}\left(-1+\left[\frac{\psi}{\psi_{\min}}\right]^{D-3}\right), \tag{19}$$

where V_T is a sample volume. Limits for the quotient $V_o/V_T=\vartheta$ are $\theta_s \leq \vartheta \leq 1$. A limit of $\vartheta=1$ corresponds to a Menger sponge with infinite recursive steps in which $V_o=V_T$ (Perrier et al., 1996). Eq. (17) is a special case in which $\vartheta=1$ but $\vartheta \neq \theta_s$. A limit of $\vartheta=\theta_s$, on the other hand, implies that $V_o=V_p$ and Eq. (19) reduces to the Brooks and Corey (1964) formulation [Eq. (15) with an exponent of $D-3$]. Thus, Eqs. (15) and (17) are particular cases of a more general Eq. (19). Eq. (15) results in lower values of D than Eq. (17) (Perrier et al., 1996; Perfect et al., 1997). Parameters ϑ and D of the Perrier et al. (1996) model are not independent and often the equation does not converge or it results in values of $\vartheta>1$, which are physically impossible (Perrier et al., 1996; Perfect et al., 1997).

Another way to look at V_o is to consider it in relation to sample size – note that the definition of V_o [Eq. (18)] contains the constant A from Eq. (12). At a fixed V_o, decreasing sample sizes may not statistically represent a fractal porous medium (Brakensiek and Rawls, 1992; Tyler and Wheatcraft, 1992b). From that perspective, V_o is a representative elementary volume (REV; Bear, 1972).

Perfect et al. (1996, 1997), using a similar model to that of Rieu and Sposito (1991a), introduced a parameter that represented a pressure potential needed to drain the smallest pores present in a Menger sponge, $\psi_{\max}$. Their formulation is (Perfect et al., 1997):

$$S_e \approx \theta/\theta_s=\left[\psi_i^{D-3}-\psi_{\max}^{D-3}\right]\Big/\left[\psi_{\min}^{D-3}-\psi_{\max}^{D-3}\right] \tag{20}$$

This equation, with $D-3=-c$, was proposed by Ross et al. (1991) as an empirical alternative to Eq. (15). Perfect et al. (1996, 1997) fitted Eq. (20) to soil-water retention data from six soils. A detailed comparison for one of the soils showed that Eq. (15) (with D-3 as the exponent) and Eq. (17) underpredicted water content at low and high pressure potentials. Eq. (20), on the other hand, provided a better fit to the soil-water retention data without bias over the range of pressure potentials considered. Values for D, however, were in the range 2.91–4.37, with 91% of the D values greater than 3. Values of $D>3$ are not physically meaningful and imply that some of the assumptions of the model are wrong or that the soils used were not mass fractal. For a mass fractal porous medium the water retention curve is concave when plotted in a semi-log scale (Fig. 3). Typically, a concave soil-water retention curve corresponds to a coarse-textured soil in contrast with fine textured soils, which produce a convex curve (Fig. 3). An alternative explanation is that fine-textured soils tend to be surface fractal.

de Gennes (1985) derived a soil-water retention model from two models of surface fractals: iterative pits (self-similar pits within pits) and iterative flocs (self-similar grains fused to grains). Both models resulted in a soil-water retention curve of

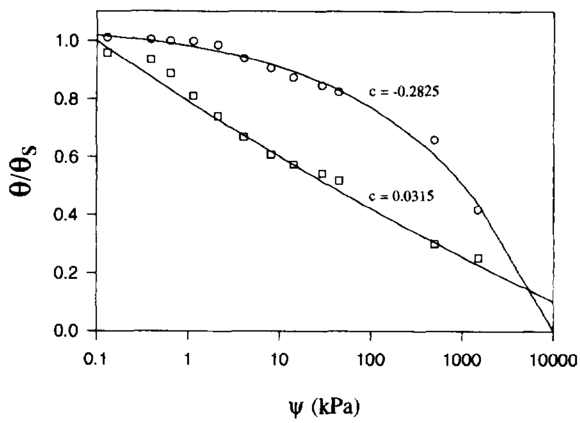

Fig. 3. Observed and predicted water retention curves for two soil cores from the Elora data set of Perfect et al. (1996) giving a positive and negative estimate of D when fitted with Eq. (20). Parameter estimates for the convex curve (circles) are: $\psi_{\min}=4\times10^{-1}$ kPa, $\psi_{\max}=1\times10^4$ kPa and $D=3.28$. Parameter estimates for the concave curve (squares) are: $\psi_{\min}=1\times10^{-1}$ kPa, $\psi_{\max}=5\times10^4$ kPa and $D=2.97$.

the form:

$$\theta=\theta_s\left(\frac{\psi}{\psi_{min}}\right)^{D_s-3}. \quad (21)$$

Eq. (21) is identical in form to Eq. (15), but in this case, the exponent is D_s. Davis (1989) found that a fit of Eq. (21) to water retention data for Berea sandstone in the range 0.7–9.4 MPa gave a $D_s=2.55$ (coefficient of determination ~ 1.00). In that range of pressure potentials, water was probably present in pockets of water connected through films (Davis, 1989). Pape et al. (1987) developed a model similar to the de Gennes (1985) model in which a pore surface is an ideal fractal, but pore volume is a nonideal fractal (Rigaut, 1984). According to this model, the graph of log θ versus log ψ is curvilinear and approaches asymptotically the constant value of θ_s. This concept is interesting because an asymptotic approaching to a constant at one or both ends of a soil-water retention provides more flexibility to a model of soil-water retention (van Genuchten and Nielsen, 1985).

Pachepsky et al. (1995b) also noted that equations derived from Eq. (12) do not perform well at both low and high pressure potentials. They proposed to replace the constant A in Eq. (12) by a probability integral function, $f(r)$, of the form:

$$f(r)=\frac{1}{\sqrt{2\pi}\sigma}\exp\left[-\frac{(\ln r-\ln\bar{r})^2}{2\sigma^2}\right], \quad (22)$$

where σ and $\bar{r}$ are the variance and geometric mean radius of a log-normal distribution of pores, respectively. Eq. (22) was selected because it predicted satisfactorily soil-water retention of fine-textured soils. Their final equation relating volumetric water content and pressure potential is:

$$\theta=\frac{\theta_o}{2}\,\mathrm{erfc}\left(\frac{1}{\sigma\sqrt{2}}\ln\frac{\psi}{\psi^*}\right), \quad (23)$$

where θ_o is a matching water content and ψ^* is the pressure potential at $\theta_o/2$. According to the derivation procedure the following relations should be obtained:

$$\ln\theta_o=\ln(\bar{r}A)+\frac{(3-D)^2}{2}\sigma^2, \quad (23a)$$

$$\ln r^*=\ln\bar{r}+(3-D)\sigma^2. \quad (23b)$$

Pachepsky et al. (1995b) found that both Eqs. (23a) and (23b) gave similar fractal dimensions for two soils and they concluded that the variance of the pore size distribution σ was an important variable that increases the precision in a determination of a water retention curve. Variance of a pore-size distribution also depends on the volume sampled according to the concept of a representative elementary volume (REV).

Tyler and Wheatcraft (1989) used the D_f from primary particles to estimate a soil-water retention curve according to the model of Arya and Paris (1981). In their original work, Arya and Paris (1981) divided a cumulative particle-size distribution into a number of fractions. For each fraction, pore volume was calculated from the mass in the fraction and the bulk density, which was assumed constant and equal to the bulk density of the structured soil. Pore volume was represented by a single cylindrical pore with a radius related to particle size and pore length. Pore length was approximated by the number of particles lying along a pore-wall multiplied by particle diameter. By acknowledging that soil particles are not spherical, they increased the number of particles in each fraction by raising it to a power >1. Tyler and Wheatcraft (1989) showed that the empirical parameter of Arya and Paris (1981) was the fractal dimension of the pore-wall, D_s. They further assumed that $D_s=D_f$ - 1 and estimated D_f from the particle size distribution. Since bulk density is constant and pore-wall is fractal, Tyler and Wheatcraft (1989) modeled the soil-water retention curve as a surface fractal in a way consistent with the model of Crawford et al. (1993b). In a later paper, Tyler and Wheatcraft (1992a) revisited the method used to calculate D_f and showed that fractal scaling is only applicable to a limited number of textural classes. Recently, Kozak et al. (1996) analyzed 2600 samples to conclude that only 20% of the samples exhibited fractal scaling of particle size distributions. Given the uncertainties in the fractal scaling of particle size distributions, present models of soil-water retention based only on D_f are not recommended. Kravchenko and Zhang (1997) modified the model of Tyler and Wheatcraft (1989) to account for a fractal distribution of mass. They also assumed

$D_s = D_f - 1$, but estimated D_f from an aggregate size distribution. This model is an improvement over the earlier model of Tyler and Wheatcraft (1989), but the assumed relationship between D_f, from an aggregate size distribution, and D_s should be taken cautiously (Crawford et al., 1993b).

All previous models represent a soil-water retention curve as a simple power law with the slope related to a fractal dimension, to correspond with the model of Campbell (1974). Empirical models often require more than one exponent to fit a soil-water retention curve in the complete range of saturation (van Genuchten and Nielsen, 1985; Ross et al., 1991). More than one fractal dimension, or even a combination of models, could be needed to fit the entire curve from saturation to dryness.

Since Eqs. (15) and (21) have the same form, a power-law could fit the entire range of soil-water contents, with a possible change in the value of the exponent D. This concept is supported by the observation that more than one fractal dimension has been reported when Eq. (13) was fitted to mercury porosimetry data (Friesen and Laidlaw, 1993; Pachepsky et al., 1995b). The D corresponding to each segment may have a different physical interpretation. Soil-water retained in small pores is likely to be a function of pore surface roughness (Bartoli et al., 1992; Jaroniec et al., 1993), whereas water retained in larger pores is probably a function of both pore size and pore roughness. Holden (1995) found that the surface fractal dimension of soil aggregates was highly correlated with soil-water retained at pressure potentials between -0.5 to -10 kPa, with the highest correlation for water retained at -10 kPa (coefficient of determination ~ 0.9). Fractal dimensions of surface roughness and pore volume are expected to be similar only for small pores (Roberts, 1986). Therefore, scaling of soil-water retention at low pressure potentials could be a function of both pore size distribution and pore roughness, each characterized by its own value of fractal dimension.

Bird et al. (1996) have shown that a soil-water retention curve with a non-power-law form can be obtained by generating a Cantor set with two scaling parameters (irregular fractals). Models derived from irregular fractals could be more flexible and provide a better fit to soil-water retention curves than a simple power-law model.

3.2. Hydraulic conductivity

Formulations for dependencies of unsaturated conductivity on pressure potential, $k(\psi)$, or on water content, $k(\theta)$, most often follow from a model of a soil-water retention characteristic (van Genuchten and Nielsen, 1985). Using the method of Mualem (1976), one can obtain the relative conductivity function for Eq. (15), with $3-D$ as the exponent:

$$k(\theta) = \theta^{2/(3-D)+2+\alpha}, \tag{26}$$

where α is a pore-interaction parameter that accounts for pore connectivity and tortuosity of the flow path, with a suggested value of $\alpha = 0.5$ (Mualem, 1976). van Genuchten et al. (1989), however, found values of α between -10 and 10 for different structured soils. The large range of variation of α suggest that D alone is not sufficient to characterize the properties of a porous medium important to flow.

Toledo et al. (1990) modeled soil-water retention and unsaturated hydraulic conductivity using fractal geometry and thin-film physics. They showed that Eq. (21) is applicable to pendular structures occupying the corners of a Menger sponge. The unsaturated hydraulic conductivity at low water content is (Toledo et al., 1990):

$$k(\theta) \propto \theta^{3/m(3-D_s)}, \tag{27}$$

where m ($1 \le m \le 3$) is a parameter that depends on the forces acting on the solid–liquid pair and D_s is the fractal dimension of pore surface obtained from a water retention curve [Eq. (21)]. The key assumption in this model is that thin films control flow and therefore predictions should be restricted to low water contents. The model predicts that for a given θ and m, the larger the D_s the larger the $k(\theta)$, corresponding to the general observation that clay soils have larger unsaturated k than coarser soils at low water contents.

Shepard (1993) used a Koch curve to model pore length (tortuosity). He assumed that the length of a straight segment in a Koch curve, r_i [Fig. 1(b)] was equal to pore diameter, d.

Tortuosity is a function of the quotient L/d, where L is the internal length of a capillary tube with diameter d representing all pores with that diameter. An average pore radius is defined as the arithmetic mean of two pressure potentials, converted to values of radius with the Young–Laplace equation. The change in water content associated with an average pore radius is obtained from the water retention curve from which the hydraulic conductivity function will be calculated. The internal pore length for an average pore radius is defined from the relationship: L_i=(pore volume)/(pore area), where pore volume is equal to the change in water content and pore area is the cross-sectional area of a circular pore with an average radius. Total number of pores, PN_i is obtained by dividing L_i by path length, PL_i, defined as $PL_i=(N/b)^i$, where N is the number of segments in the generator [Fig. 1(b)], $b=3$ and i is the generation number of the Koch curve. The generation number is determined from the unit length of the straight segments of a Koch curve as $r_i=1/b^i$, where r_i is calculated from the equality $r_i=d_i$. Poiseuille's equation is used to calculate the volume flux, q_i, through a pore with radius $d/2$ and associated path length PL_i. Total flux Q_i is calculated as $Q_i=q_iPN_i$ and the hydraulic conductivity is calculated as the summation of Q_i over the different pore classes considered. Note that PL_i is related to the fractal dimension of the Koch curve, i.e. $PL_i=(b^{D-1})^i$. Assuming that b is equal to particle diameter, the expression to calculate path length in Shepard (1993) is identical to the one presented by Tyler and Wheatcraft (1989). Interestingly, using this approach the fractal dimensions of pore surface were almost constant, with an average of $D_s=1.22$, for soils with different textures. This suggests that the relationship between pore and particle diameters is similar throughout soils. Variability among soils is in the total length of pores in each class, which is related to the distribution of pore volume in each class.

Fuentes et al. (1996) used D, obtained from a soil-water retention curve, to derive an expression for $k(\theta)$. Characterizing the soil-water retention curve as $\theta \propto \psi^{D-3}$, $k(\theta)$ can be expressed as:

$$k(\theta) \propto \theta^{2/(3-D)+2D/3} \quad (28)$$

Fuentes et al. (1996) relate D to total porosity ϕ as:

$$(1-\phi)^{D/3}+\phi^{2/3D}=1, \quad (29)$$

where $(1-\phi)^{D/3}$ is the area occupied by the solid and $\phi^{2/3D}$ is the minimum area available participating in the flow. Fuentes (1992) showed that the expression for minimum area available can be derived from probabilistic considerations in agreement with the Millington and Quirk (1961) model. For the porosity values between 0.3 and 0.6 often found in soils, Fuentes et al. (1996) concluded that D can only vary between 2 and 2.2. A comparison between the theoretical range of values for D and those in Tables 1–3 show, however, that the theoretical range is extremely narrow when compared with the measured ones. Consequently, the morphological interpretation of D in the Fuentes et al. (1996) model is not clear.

Rieu and Sposito (1991a) also calculated an unsaturated hydraulic conductivity function based on the water retention curve and aggregate-size distribution. The model requires information on the similarity ratio b, a fractal dimension of the fragmented medium, D_f and a fractal dimension of the incompletely fragmented soil, D_{if}. Pressure potential and the scaling ratio b are related by $b^{i}=\psi_i/\psi_{min}$. Thus, a plot of $\log(\psi_i/\psi_{min})$ vs an arbitrary integer scale is a straight line with a slope of $\log b$. The fractal dimension D_f is obtained from the aggregate size distribution and D_{if} from the water retention curve. Their expression is:

$$k_i=C\beta_r \sum_{j=1}^{n-1} (d_f)_j^2 G^j, \quad (30)$$

where C is a constant that depends on pore geometry and fluid properties, β_r and G are the two-dimensional analogs of Γ_r and F, respectively and $(d_f)_j$ is the vertically oriented fracture opening. The parameter G^j accounts for a reduction in connectivity. The two-dimensional analogs G and β_r are obtained from the three-dimensional variables by assuming an area:volume ratio of 2:3. For a Menger sponge, however, $D_s=D_v$ and the area:-volume ratio is unity. In addition, the model assumes that F (or G) remains constant with aggregate size. A size-variant F will produce different values of D for different levels of applied energy input (Perfect and Kay, 1995a). Nevertheless, the model predicted the unsaturated hydraulic conductivity function of a silty clay loam reasonably well (Rieu and Sposito, 1991b).

Crawford (1994) developed expressions for the $k(\psi)$ that incorporated a mass fractal dimension, D_m, and a spectral dimension, $\bar{d}$, of the solid random fractal matrix to represent soil structural heterogeneity and pore wall shape, respectively. Using $\theta \propto \psi^{D_m-3}$ as an expression for a soil-water retention, a $k(\theta)$ function can be written as:

$$k(\theta) \propto \theta^{[1/(D_m-3)](\xi-1)[3+2(D_m/\bar{d})-D_m]}, \tag{31}$$

where ξ is an undetermined function of soil structure with values <1. Since $\bar{d}=D_m/D_w$, and for this system $D_s=D_w$, Eq. (31) reduces to:

$$k(\theta) \propto \theta^{[1/(D_m-3)](\xi-1)[3+2D_s-D_m]}, \tag{32}$$

which shows that $k(\theta)$ is a function of the irregularities of a pore-solid interface and of the distribution of mass. The dependence of ξ on θ, D_m and $\bar{d}$ needs to be investigated.

In general, predictions of $k(\theta)$ are sensitive to the value of D, which in all cases is derived from a soil-water retention curve, $\theta(\psi)$. For instance, fitting an equation of the form $k(\theta) \propto \theta^M$ to the data in Rieu and Sposito (1991b) gives: $k(\theta) \propto \theta^{29.25}$. Using $D_m=2.90$, obtained by Rieu and Sposito (1991b) by applying Eq. (17) to the soil-water retention of their soil and assuming $\xi=0.5$, the exponent in Eq. (32) yields an estimate of $D_s=2.87$, which is theoretically possible. If, on the other hand, a soil-water retention model of the form assumed by Crawford (1994) [Eq. (15)] is fitted to the data, a D_m value of 2.71 is obtained (Perrier et al., 1996), which now gives a physically meaningless estimate of $D_s=8.34$ when $\xi=0.5$. This example shows that an understanding of the effect of the geometry of porous media on the flow process is essential to a correct determination of any parameter of soil structure.

Another important hydraulic property is the saturated hydraulic conductivity, k_{sat}. Despite similarities between the $k(\theta)$-θ and k_{sat}-porosity functions, formulations for k_{sat} were typically developed independently of any $\theta(\psi)$ and/or $k(\theta)$ model. Models of k_{sat} are derived from the Kozeny–Carman and Marshall (1958) models. The Kozeny–Carman equation (Giménez et al., 1997b) is:

$$k_{sat} = C_o \phi / T S_a^2, \tag{33}$$

where C_o is a constant that depends on pore shape, ϕ is porosity and T is a tortuosity factor often defined as $(L_e/L)^2$, where L_e and L are the apparent and actual flow path lengths, respectively (Epstein, 1989) and S_a is the specific surface area expressed per unit pore volume.

Adler and Thovert (1992) reported extensive numerical experiments on flow in deterministic fractal structures. Navier–Stokes equations were solved for one-, two- and three-dimensional geometries. Using a Sierpinski carpet as a model, they reported that for the one-dimensional case, results were consistent with a generalized Kozeny–Carman equation (Jacquin and Adler, 1987):

$$k_{sat} \propto \phi^{\mu}, \tag{34}$$

where μ is a function of the fractal dimension D. The relationship between D and μ is a function of the model used (Table 4). Jacquin and Adler (1987) derived μ for a Sierpinski carpet, whereas Muller and McCauley (1992) derived μ from a simplified "fractal tree". The main difference is that in the model of Jacquin and Adler (1987) flow is dominated by the larger pores, whereas in the model of Muller and McCauley (1992), smaller pores are controlling the flow. Probably, a real porous medium is somewhere in between these two extremes. Korvin (1992b) derived a different form of the exponent μ by expressing the surface area and tortuosity in the Kozeny–Carman model in a fractal form.

Table 4
Forms of the exponent μ of Eq. (34) determined from fractal models

N	Reference
$(4-D)/(2-D)$[a]	Jacquin and Adler (1987)
$(4-D_v)/D_v$	Muller and McCauley (1992)
$(D-1)/(3-D)$[b]	Korvin (1992a)
$2[(2-D_s)/(3-D_v)]+3+\alpha$	Giménez et al. (1997b)

[a]Sierpinski carpet; Fig. 1(c), with black area representing pore space.
[b]values of D_s and D_v assumed equal.

The connectivity of the pore system and the type of porosity also influence the k_{sat}–ϕ relationship. Hansen and Muller (1992) used mean field theory to calculate an effective k_{sat} for a porous medium with uniform fractal scaling of pore space. They showed that a highly connected pore system is less sensitive to a decrease in ϕ than a poorly connected one. Ahuja et al. (1984) used an effective porosity in Eq. (34) to predict k_{sat}. Effective porosity was defined as the porosity between saturation and a pressure potential of -33 kPa. This definition seems somewhat arbitrary; but, in general, better predictions are obtained with Eq. (34) in the form $k_{sat} \propto \phi_m^{\mu}$, where ϕ_m is a porosity corresponding to the larger pores (macroporosity).

Hansen and Skjeltorp (1988) derived a fractal form for the Kozeny–Carman equation using a volume filling procedure by which particles of increasingly smaller size are packed in a given initial volume. They considered a reduction in pore volume and an increase in surface area from the addition of particles of subsequently smaller size. They further assumed that the resulting pore volume and pore surface were fractal and used these results to calculate a specific surface area, S_a, as:

$$S_a \propto (\ell_{max}/\ell_{min})^{(D_s-2)+(3-D_v)}, \tag{35}$$

where ℓ_{max} and ℓ_{min} are the upper and lower limits of fractal scaling. Introducing Eq. (35) in a Kozeny–Carman model results in:

$$k_{sat} \propto \phi(\ell_{max}/\ell_{min})^{2[(2-D_s)+(D_v-3)]}, \tag{36}$$

This model implicitly incorporates tortuosity into the fractal dimensions D_s and D_v. Note that at a fixed porosity and quotient ℓ_{max}/ℓ_{min}, Eq. (36) predicts lower k_{sat} values for higher values of D_s and lower values of D_v. This seems to be a problem since fine textured soils tend to have higher D_v values (Brakensiek and Rawls, 1992; Rieu and Sposito, 1991b) and lower k_{sat} values (Rawls et al., 1982). Giménez et al. (1997b) modified Eq. (36) by considering the scaling of S_a in a system composed by an originally solid block in which pores of increasingly smaller sizes are opened between limits $\ell_{min} \le \ell \le \ell_{max}$. Their expression is:

$$k_{sat} \propto \phi(\ell_{max}/\ell_{min})^{2[(2-D_s)+(3-D_v)]}, \tag{37}$$

which now predicts a decrease in k_{sat} with higher D_s and higher D_v values. This expression was tested with data on ϕ_m and k_{sat} reported in Logsdon et al. (1990) and supplemented with maximum pore radius, r_1 and D_v data reported by Rawls et al. (1993) and Brakensiek et al. (1992), respectively (Table 5). It was assumed that the characteristic size ℓ [Eqs. (3a) and (3b)] was proportional to pore radius. The minimum pore radius measured by Logsdon et al. (1990) was $r_{min}=0.04$ cm and assumed constant during calculations. An estimate of D_s with Eq. (37) is 2.49 ± 0.08 for the two soils in Table 5 (Fig. 4). The same data fitted to Eq. (36) resulted in D_s values not statistically different from 2 (Giménez, 1995) and lower than expected based on measured data (Kampichler and Hauser, 1993; Anderson et al., 1996; Giménez et al., 1997a).

Giménez et al. (1997b) modified Eq. (37) to express k_{sat} as a function of ϕ_m:

$$K_{sat} \propto \phi_m^{2[(2-D_s)/(3-D_v)]+3+\alpha}, \tag{38}$$

where α is an exponent that represents tortuosity and connectivity. Comparing Eqs. (34) and (38), one can write $\mu = 2[(2-D_s)/(3-D_v)]+3+\alpha$. Fractal dimensions D_s and D_v and porosity ϕ_m were measured from images of impregnated soil, with k_{sat} measured either in the same soil volume or on samples taken from an adjacent site. Giménez et al. (1997b) fitted pairs of k_{sat}-ϕ_m values to Eq. (34) to obtain μ and used the fitted μ values together with measured D_s and D_v to calculate values of α in Eq. (38). The values of α were between 1.98 and -1.20 and were related to pore structure, expressed by the quotient $MWHR_u/MWHR_\ell$, where MWHR is a mean-weighted hydraulic radius (pore area/pore perimeter) obtained from the lower one-half ($MWHR_\ell$) and upper one-half ($MWHR_u$) of a probability distribution of hydraulic radii, weighted according to the number of pores on each portion of the distribution (Fig. 5). Giménez et al. (1997b) conjectured that better prediction of the exponent μ can be achieved by measuring scaling pore properties on only active pores.

Rawls et al. (1993) derived an equation for predicting k_{sat} based on the Marshall (1958) equation coupled with fractal properties of a Sierpinski

Table 5
Measurements of saturated hydraulic conductivity, k_{sat}, maximum macropore radius, r_1, and macroporosity, ϕ_m, for two soils in the data set of Logsdon et al. (1990)

Soil	Treatment[a]	k_{sat} (cm h^{-1})	r_1 (cm)[b]	ϕ_m ($\times 10^{-2}$)[c]	D_v[d]	D_s[e]
Clay loam	NT	3.45	0.20	0.16	2.84	
	NT	10.87	0.17	0.14	2.82	
	MB	20.41	0.18	0.20	2.82	
	CH	7.34	0.30	0.22	2.89	
	RT	12.67	0.49	0.70	2.84	
						2.49±0.08
Silt loam	NT	2.75	0.12	0.14	2.76	
	NT	19.44	0.19	0.63	2.84	
	MB	56.88	0.40	1.66	2.78	
	A	25.38	0.39	1.05	2.75	
	A	54.00	0.15	1.04	2.81	
	O	31.43	0.40	0.80	2.82	

[a]NT, no-till; MB, moldboard plow; CH, chisel plow; RT, ridge-till; A, alfalfa, O, oat.[b]Maximum pore radius from Rawls et al. (1993); minimum pore radius assumed constant with a value $r_{min}=0.04$ cm.[c]Macroporosity obtained by size-count of pores with radii >0.04 cm.[d]Fractal dimension of pore volume according to Brakensiek et al. (1992).[e]Fractal dimension of pore surface obtained by fitting Eq. (37) to data from both soils.

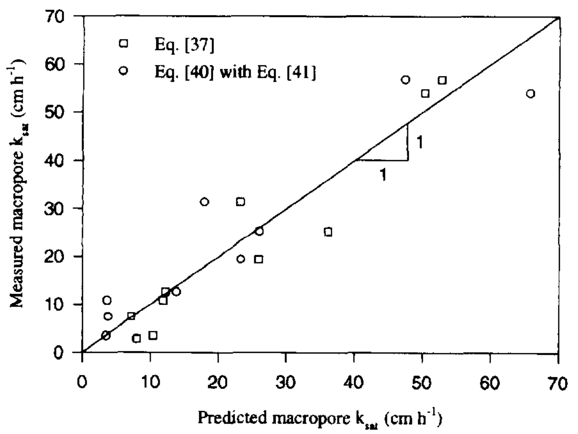

Fig. 4. Measured macropore saturated hydraulic conductivity, k_{sat}, versus predicted k_{sat} with Eq. (37), and Eqs. (40) and (41).

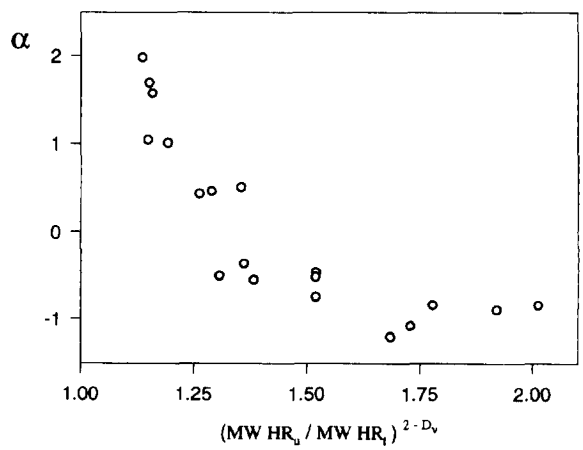

Fig. 5. Parameter α from Eq. (38) plotted as a function $(MWHR_u/MWHRt)^{2-D_v}$. For explanation see text.

carpet (Tyler and Wheatcraft, 1990). The Marshall (1958) model divides a pore size distribution into n classes, but considers that $Y<n$ classes contribute effectively to saturated flow. The ith pore size class is characterized by its pore radius, r_i. A saturated hydraulic conductivity is calculated by summing the contribution of Y classes of pore radius r_i as:

$$k_{sat}=C(\phi^x/n^2)\sum_{i=1}^{Y}(2i-1)r_i^2, \tag{39}$$

where x is a pore interaction factor defined by Millington and Quirk (1961) and C is a constant that depends on pore geometry and fluid properties ($C=4.41\times10^7$ for water at 20°C). Rawls et al. (1993) showed that $\Sigma_{i=1}^{Y}(2i-1)r_i^2=r_1^2$, where r_1^2 is the largest equivalent pore radius of the Sierpinski carpet (Tyler and Wheatcraft, 1990). Their final equation requires information on r_1, porosity ϕ, x and n:

$$k_{sat}=4.41\times10^7\phi^x(r_1^2/n^2). \tag{40}$$

Note that the pore interaction parameter x would depend on the limits of fractal behavior and on the fractal dimensions of the fractal model (Adler, 1992). Fuentes et al. (1996) expressed x as $x = 2/3D$ [see Eq. (29)]. By defining the limits of D between $2.0 \leq D \leq 2.2$ in Eq. (29), x can only vary between 4/3 and 4.4/3. As noted before, however, the limits of D may be too restrictive and more work is needed to establish the link between x and fractal parameters of soil structure.

Rawls et al. (1993) used Eq. (40) to predict k_{sat} for soils with and without large connected pores (macropores). The latter situation depends on the properties of the soil matrix (matrix-k_{sat}), whereas the former is a function of the distribution and properties of macropores (macropore-k_{sat}). Macropores are particularly important in agricultural soils subjected to no-till practices. Since $k_{sat} \propto r^2$, macropore k_{sat} can be several orders of magnitude larger than the matrix-k_{sat}. Rawls et al. (1993) predicted matrix-k_{sat} for different textures using data presented in Rawls et al. (1982). Bubbling pressure, ψ_{min}, was used to calculate r_1 [$r_1 \sim 0.15/\psi_{min}$, (cm)] and x was assumed constant and equal to 4/3 (Millington and Quirk, 1961). In addition, they defined n as:

$$n = Y\left(\frac{\phi}{\phi - \theta_l}\right),$$

where Y is 12 (Marshall, 1958) and θ_l is effective porosity defined as the porosity between saturation and pressure potential of -33 kPa (Ahuja et al., 1984). They also related n to the fractal dimension D calculated as $D = 2\text{-}\lambda$, where λ is defined in Eq. (16). Eq. (40) produced excellent results in predicting matrix-k_{sat} across textures. To test their formulation for the prediction of macropore-k_{sat}, Rawls et al. (1993) fitted Eq. (34) to the k_{sat}–ϕ_m data reported by Logsdon et al. (1990) to obtain $\mu = 4/3$. Eq. (40), with $x = \mu = 4/3$ and n as the only unknown, resulted in a good prediction of macropore-k_{sat} (Fig. 4). The estimated ns were linearly related to r_1 according to the following equation:

$$n = -5.7 + 77.0\ r_1, r = 0.93, \tag{41}$$

Independent tests showed that use of Eqs. (40) and (41) resulted in reasonable predicted values for macropore-k_{sat}. Rawls et al. (1996) extended the application of Eq. (40) for no-till soils by generating schemes to calculate macropore size/count, areal porosity and macropore conductivity based on different levels of data availability.

4. Conclusions

Experimental evidence suggests that the morphology of soil structure is fractal within some scale limits, but there is no clear understanding of the relationship among fractal dimensions of soil structure. Consequently, fractal models with contrasting assumptions are used to predict soil hydraulic properties.

Although important, applications of fractals have been limited to fitting fractal models of soil hydraulic properties to data and to discussing the physical/theoretical value of the fitted fractal dimensions. Most often, fractal models are tested with data sets collected for other purposes and are, therefore, limited in their possibilities. As a result, the morphological interpretation of the fitted fractal dimensions has not been fully explored. Further research is needed on evaluating the predictive capabilities of fractal dimensions determined independently. Concurrent measurements of fractal dimensions characterizing the geometry and connectivity of soil structure together with the soil-water retention and conductivity functions are needed to test fractal models. This approach would shed light on the fractal nature of soil structure and likely improve modeling efforts. Furthermore, an understanding of the morphological significance of the fractal dimension(s) determining a soil property (or process) is basic for creating a general framework to model soils with a set of parameters describing scaling of the basic components of soil structure.

A complete representation of a soil-water retention from saturation to dryness requires probably more than one fractal dimension to characterize different scaling regions. Fractal dimensions characterizing separate scaling domains do not necessarily have the same geometrical interpretation; e.g. under dry conditions, hydraulic properties could be mainly determined by surface area, whereas close to saturation, pore volume could be more important. Currently, $\theta(\psi)$ functions are derived from models that are mass, volume or surface fractals without consideration of connectivity or other parameters of soil structure such as lacunarity. No attempt has been made to model a $\theta(\psi)$ as a result of several fractal properties. Most fractal models of hydraulic conductivity, on the other hand, have recognized the importance of those parameters and present formulations often combine more than one fractal dimension and/or intrinsic dimensions (e.g. spectral and connectivity dimensions). Models of saturated and unsaturated hydraulic conductivity have evolved separately. There is a need to unify both approaches and link it to the modeling of soil-water retention properties.

This review has identified several different fractal models for the soil-water retention curve and the hydraulic conductivity–water content function. Detailed studies are needed to compare the performance of these different models over a range of soil types and structural conditions with data collected for that specific purpose.

Acknowledgment

We are grateful to Drs D. Brakensiek, B. Das and E. Eghball for reviewing an early version of this paper and for their useful suggestions for improvements.

References

Adler, P.M. 1992. Porous Media: Geometry and Transports. Butterworth and Heinemann, Stoneham, MA.

Adler, P.M., Thovert, J.-F., 1992. Fractal porous media. Transp. Porous Media 13, 41–78.

Ahl, C., Niemeyer, J., 1989. The fractal dimension of the pore-volume inside soils. Z. Pflanzenernahr. Bodenkd. 152, 457–458.

Ahuja, L.R., Naney, J.W., Green, R.E., Nielsen, D.R., 1984. Macroporosity to characterize spatial variability of hydraulic conductivity and effects of land management. Soil Sci. Soc. Am. J. 48, 699–702.

Anderson, A.N., McBratney, A.B., 1995. Soil aggregates as mass fractals. Aust. J. Soil Res. 33, 757–772.

Anderson, A.N., McBratney, A.B., FitzPatrick, E.A., 1996. Soil mass, surface and spectral fractal dimensions estimated from thin section photographs. Soil Sci. Soc. Am. J. 60, 962–969.

Arya, L.M., Paris, J., 1981. A physico-empirical model to predict the soil moisture characteristic from particle-size distribution and bulk density data. Soil Sci. Soc. Am. J. 45, 1023–1030.

Avnir, D., Farin, D., Pfeifer, P., 1985. Surface geometric irregularity of particulate materials: The fractal approach. J. Colloid Interface Sci. 103, 112–123.

Barak, P., Seybold, C.A., McSweeney, K., 1996. Self-similitude and fractal dimension of sand grains. Soil Sci. Soc. Am. J. 60, 72–76.

Bartoli, F., Philippy, R., Doirisse, M., Niquet, S., Dubuit, M., 1991. Structure and self-similarity in silty and sandy soils: the fractal approach. J. Soil Sci. 42, 167–185.

Bartoli, F., Philippy, R., Burtin, G., 1992. Influence of organic matter on aggregation in Oxisols rich gibbsite or in goethite. I. Structures: the fractal approach. Geoderma 54, 231–257.

Bartoli, F., Burtin, G., Philippy, R., Gras, F., 1993. Influence of fir root zone on soil structure in a 23 m forest transect: the fractal approach. Geoderma 56, 67–85.

Bear, J., 1972. Dynamics of Fluid Flow in Porous Media. Elsevier, New York.

Bird, N.R.A., Bartoli, F., Dexter, A.R., 1996. Water retention models for fractal soil structures. Eur. J. Soil Sci. 47, 1–6.

Borkovec, M., Wu, Q., Degovics, G., Laggner, P., Sticher, H., 1993. Surface area and size distributions of soil particles. Colloids Surf. A: Physicochem. Eng. Aspects 73, 65–76.

Brakensiek, D.L., Rawls, W.J., 1992. Comment on "Fractal Processes in Soil Water Retention" by S.W. Tyler and S.W. Wheatcraft. Water Resourc. Res. 28, 601–602.

Brakensiek, D.L., Rawls, W.J., Logsdon, S.D., Edwards, W.M., 1992. Fractal description of macroporosity. Soil Sci. Soc. Am. J. 56, 1721–1723.

Brooks, R.H., Corey, A.T., 1964. Hydraulic Properties of Porous Media. Hydrology Paper 3, Colorado State University, Fort Collins.

Campbell, G.S., 1974. A simple method for determining unsaturated conductivity from moisture retention data. Soil Sci. 117, 311–314.

Chepil, W.S., 1950. Methods of estimating apparent density of discrete soil grains and aggregates. Soil Sci. 70, 351–362.

Clapp, R.B., Hornberger, G.M., 1978. Empirical equations for some soil hydraulic properties. Water Resourc. Res. 14, 601–604.

Crawford, J.W., 1994. The relationship between structure and the hydraulic conductivity of soil. Eur. J. Soil Sci. 45, 493–501.

Crawford, J.W., Ritz, K., Young, I.M., 1993a. Quantification of fungal morphology, gaseous transport and microbial dynamics in soil: an integrated framework utilizing fractal geometry. Geoderma 56, 157–172.

Crawford, J.W., Sleeman, B.D., Young, I.M., 1993b. On the relation between number–size distribution and the fractal dimension of aggregates. J. Soil Sci. 44, 555–565.

Crawford, J.W., Matsui, N., Young, I.M., 1995. The relation

between the moisture-release curve and the structure of soil. Eur. J. Soil Sci. 46, 369–375.
Crawford, J.W., Matsui, N., 1996. Heterogeneity of the pore and solid volume of soil: distinguishing a fractal space from its nonfractal complement. Geoderma 73, 183–195.
van Damme, H., 1995. Scale invariance and hydric behavior of soils and clays. C.R. Acad. Sci. Paris 320, 665–681.
Davis, H.T., 1989. On the fractal character of the porosity of natural sandstone. Europhys. Lett. 8, 629–632.
de Gennes, P.G., 1985. Partial filling of a fractal structure by a wetting fluid. In: Adler, D., Frietzsche, E., Ovshinsky, S.R., (Eds.), Physics of Disordered Materials. Plenum Press, New York, pp. 227–241.
Dexter, A.R., 1988. Advances in characterization of soil structure. Soil Tillage Res. 11, 199–238.
Dirksen, C., 1991. Unsaturated Hydraulic Conductivity. In: Smith,. K.A., Mullins, C.E. (Eds.), Soil Analysis Physical Methods. Dekker, New York, pp. 209–269.
Eghball, B., Mielke, L.N., Calvo, G.A., Wilhelm, W.W., 1993. Fractal description of soil fragmentation for various tillage methods and crop sequences. Soil Sci. Soc. Am. J. 57, 1337–1341.
Epstein, N., 1989. On tortuosity and the tortuosity factor in flow and diffusion through porous media. Chem. Eng. Sci. 44 (3), 777–779.
Feder, J., 1988. Fractals. Plenum Press, New York.
Friesen, W.I., Mikula, R.J., 1987. Fractal dimensions of coal particles. J. Colloid Interface Sci. 120, 263–271.
Friesen, W.I., Laidlaw, W.G., 1993. Porosimetry of fractal surfaces. J. Colloid Interface Sci. 160, 226–235.
Fuentes, C., 1992. Approache fractale des transferts hydriques dans les sols nonsaturés. Ph.D. thesis. University of Grenoble, France.
Fuentes, C., Vauclin, M., Parlange, J-I., Haverkamp, R., 1996. A note on the soil-water conductivity of a fractal soil. Transp. Porous Media 23, 31–36.
Giménez, D., 1995. Functional characterization of soil structure: the fractal approach. Ph.D. dissertation. University of Minnesota, St Paul, MN.
Giménez, D., Allmaras, R.R., Huggins, D.R., Nater, E.A., 1994. Fractal characterization of tilled layers to predict saturated hydraulic conductivity. Proceedings of the 13th International Conference, International Soil Tillage Research Organization, Aalborg, Denmark, pp. 555–560.
Giménez, D., Allmaras, R.R., Nater, E.A., Huggins, D.R., 1997a. Fractal dimensions for volume and surface of interaggregate pores: scale effects. Geoderma 77, 19–38.
Giménez, D., Allmaras, R.R., Huggins, D.R., Nater, E.A., 1997b. Prediction of the saturated hydraulic conductivity-porosity dependence using fractals. Soil Sci. Soc. Am. J. 61, 1285–1292.
Ghilardi, P., Kai Kai, A., Menduni, G., 1993. Self-similar heterogeneity in granular porous media at the representative elementary volume scale. Water Resourc. Res. 29, 1205–1214.
Ghilardi, P., Menduni, G., 1996. Scaling properties of porous media with power-law particle size distribution. J. Hydrol. 187, 223–236.
Glasbey, C.A., 1995. Non-Fickian diffusion. Eur. J. Soil Sci. 46, 159
Gouyet, J.-F., 1996. Physics and Fractal Structures. Springer, New York.
van Genuchten, M.Th., 1980. A closed form equation for predicting the hydraulic conductivity of unsaturated soils. Soil Sci. Soc. Am. J. 44, 892–898.
van Genuchten, M.Th., Nielsen, D.R., 1985. On describing and predicting the hydraulic properties of unsaturated soils. Annals Geophys. 3, 615–628.
van Genuchten, M.Th., Kaveh, F., Russell, W.B., Yates, S.R., 1989. Direct and indirect methods for estimating the hydraulic properties of unsaturated soils. In: Bouma, J., Bregt, A.K. (Eds.), Land Quality in Space and Time. Pudoc, Wageningen, pp. 61–72.
Guerrini, I.A., Swartzendruber, D., 1994. Fractal characteristics of the horizontal movement of water in soil. Fractals 2, 465–468.
Hadas, A., 1987. Long-term tillage practice effects on soil aggregation modes and strength. Soil Sci. Soc. Am. J. 51, 191–197.
Hansen, J.P., Muller, J., 1992. Mean field calculation of effective permeability based on fractal pore space. Transp. Porous Media 8, 93–97.
Hansen, J.P., Skjeltorp, A.T., 1988. Fractal pore space and rock permeability implications. Phys. Rev. B 38, 2635–2638.
Hardy, H.H., Beier, R.A., 1994. Fractals in Reservoir Engineering. World Scientific, Singapore.
Holden, N.M., 1995. Temporal variation in ped shape in an old pasture soil. Catena 24, 1–11.
Jacquin, C.G., Adler, P.M., 1987. Fractal porous media II: geometry of porous geological structures. Transp. Porous Media 2, 571–596.
Jaroniec, M., Gilpin, R.K., Choma, J., 1993. Correlation between microporosity and fractal dimension of active carbons. Carbon 31, 325–331.
Kampichler, C., Hauser, M., 1993. Roughness of soil pore surface and its effect on available habitat space of microarthropods. Geoderma 56, 223–232.
Katz, A.J., Thompson, A.H., 1985. Fractal sandstone pores: implication for conductivity and pore formation. Phys. Rev. Lett. 54, 1325–1328.
Korvin, G., 1992a. Fractal Models in the Earth Sciences. Elsevier, Amsterdam.
Korvin, G., 1992b. A percolation model for the permeability of kaolinite-bearing sandstones. Geophys. Trans. 37, 177-209.
Kozak, E., Pachepsky, Ya., Sokolowski, S., Sokolowska, Z., Stepniewski, W., 1996. A modified number-based method for estimating fragmentation fractal dimensions of soils. Soil Sci. Soc. Am. J. 60, 1291–1297.
Kravchenko, A.N., Zhang, R., 1997. Estimation of soil water retention function from texture and structure data: fractal approach. In: Novak, M.M, Dewey, T.G. (Eds.), Fractal Frontiers. World Scientific, Singapore, pp. 329–338.

Krohn, C.E., 1988. Fractal measurements of sandstones shales and carbonates. J. Geophys. Res. 93, 3297–3305.

Larson, W.E., Padilla, W.A., 1990. Physical properties of a Mollisol, an Oxisol and an Inceptisol. Soil Tillage Res. 16, 23–33.

Lin, S., 1971. Porosity and pore-size distribution of soil aggregates. Bulletin 29, WRRC, MN.

Logsdon, S.D., Allmaras, R.R., Wu, L., Swan, J.B., Randall, G.W., 1990. Macroporosity and its relation to saturated hydraulic conductivity under different tillage practices. Soil Sci. Soc. Am. J. 54, 1096–1101.

Logsdon, S., Giménez, D., Allmaras, R.R., 1996. Fractal characterization of aggregate-size distribution: The question of self invariance. Soil Sci. Soc. Am. J. 60, 1327–1330.

Mandelbrot, B.B., 1983. The Fractal Geometry of Nature. W.H. Freeman, San Francisco, CA.

Marshall, T.J., 1958. A relationship between permeability and size distribution of pores. J. Soil Sci. 9, 1–8.

McBratney, A.B., 1993. Comments on "Fractal dimensions of soil aggregate-size distribution calculated by number and mass". Soil Sci. Soc. Am. J. 57, 1393

Millington, R.J., Quirk, J.P., 1961. Permeability of porous solids. Trans. Faraday Soc. 57, 1200–1206.

Mualem, Y., 1976. A new model for predicting the hydraulic conductivity of unsaturated porous media. Water Resourc. Res. 12, 513–522.

Muller, J., McCauley, J.L., 1992. Implication of fractal geometry for fluid flow properties of sedimentary rocks. Transp. Porous Media 8, 133–147.

Nagahama, H., 1993. Fractal fragment size distribution for brittle rocks. Int. J. Rock Mech. Min. Sci. Geomech. Abstr. 30, 469–471.

Neimark, A., 1992. A new approach to the determination of the surface fractal dimension of porous solid. Physica A 191, 258–262.

Onoda, G.Y., Toner, J., 1986. Fractal dimensions of model particle packings having multiple generations of agglomerates. J. Am. Ceram. Soc. 69, C278–C279.

Ozhovan, M.I., Dmitriev, I.E., Batyukhnova, O.G., 1993. Fractal structure of pores in clay soil. Moscow Scientific and Industrial Association "Radon". Atomnaya Energiya 74 (3), 256–258.(translated from Russian)

Pachepsky, Y.A., Polubesova, T.A., Hajnos, M., Sokolowska, Z., Jozefaciuk, G., 1995a. Fractal parameters of pore surface area as influenced by simulated soil degradation. Soil Sci. Soc. Am. J. 59, 68–74.

Pachepsky, Y.A., Shcherbakov, R.A., Korsunskaya, L.P., 1995b. Scaling of soil water retention using a fractal model. Soil Sci. 159, 99–104.

Pachepsky, Y.A., Korsunskaia, L.P., Hajnos, M., 1996a. Fractal parameters of soil pore surface area under a developing crop. Fractals 4, 97–104.

Pachepsky, Y.A., Yakovchenko, V., Rabenhorst, M.C., Pooley, C., Sikora, L., 1996b. Fractal parameters of pore surface as derived from micromorphological data: effect of long-term management practices. Geoderma 74, 305–320.

Pape, H., Riepe, L., Schopper, J.R., 1987. Interlayer conductivity of rocks — a fractal model of interface irregularities for calculating interlayer conductivity of natural porous mineral systems. Colloids Surf. 27, 97–122.

Perfect, E. 1997. Fractal models for the fragmentation of rocks and soils: a review. Eng. Geol. (this issue).

Perfect, E., Kay, B.D., 1991. Fractal theory applied to soil aggregation. Soil Sci. Soc. Am. J. 55, 1552–1558.

Perfect, E., Rasiah, V., Kay, B.D., 1992. Fractal dimensions of soil aggregate-size distributions calculated by number and mass. Soil Sci. Soc. Am. J. 56, 1407–1409.

Perfect, E., Kay, B.D., Rasiah, V., 1993. Multifractal model for soil aggregate fragmentation. Soil Sci. Soc. Am. J. 57, 896–900.

Perfect, E., Kay, B.D., 1995a. Applications of fractals in soil and tillage research: a review. Soil Tillage Res. 36, 1–20.

Perfect, E., Kay, B.D., 1995b. Brittle fracture of fractal cubic aggregates. Soil Sci. Soc. Am. J. 59, 969–974.

Perfect, E., McLaughlin, N.B., Kay, B.D., Topp, G.C., 1996. An improved fractal equation for the soil water retention curve. Water Resourc. Res. 32, 281–287.

Perfect, E., McLaughlin, N.B., Kay, B.D., Topp, G.C., 1997. Reply to comments on "An improved fractal equation for the soil water retention curve". Water Resourc. Res. (in review).

Perrier, E., Rieu, M., Sposito, G., de Marsily, G., 1996. Models of the water retention curve for soils with a fractal pore size distribution. Water Resourc. Res. 32, 3025–3031.

Peyton, R.L., Gantzer, C.J., Anderson, S.H., Haeffner, B.A., Pfeifer, P., 1994. Fractal dimension to describe soil macropore structure using X ray computed tomography. Water Resourc. Res. 30, 691–700.

Pfeifer, P., Avnir, D., 1983. Chemistry in noninteger dimensions between two and three. I. Fractal theory of heterogeneous surfaces. J. Chem. Phys. 79, 3558–3565.

Rasiah, V., Kay, B.D., Perfect, E., 1993. New mass-based model for estimating fractal diemensions of soil aggregates. Soil Sci. Soc. Am. J. 57, 891–895.

Rawls, W.J., Brakensiek, D.L., Saxton, K.E., 1982. Estimation of soil water properties. Trans. ASAE 25, 1316–1328.

Rawls, W.J., Brakensiek, D.L., Logsdon, S.D., 1993. Predicting saturated hydraulic conductivity utilizing fractal principles. Soil Sci. Soc. Am. J. 57, 1193–1197.

Rawls, W.J., Brakensiek, D.L., Logsdon, S.D., 1996. Estimation of macropore properties for no-till soils. Trans. ASAE 39, 91–95.

Rieu, M., Sposito, G., 1991a. Fractal fragmentation, soil porosity and soil water properties: I. Theory. Soil Sci. Soc. Am. J. 55, 1231–1238.

Rieu, M., Sposito, G., 1991b. Fractal fragmentation, soil porosity and soil water properties: II. Applications. Soil Sci. Soc. Am. J. 55, 1239–1244.

Rieu, M., Sposito, G., 1991c. The water characteristic curve of fragmented porous media and the fractal nature of soil structure. C.R. Acad. Sci. Paris (Ser. II) 312, 1483–1489.

Rigaut, J.P., 1984. An empirical formulation relating boundary lengths to resolution in specimens showing "non-ideally fractal" dimensions. J. Microsc. 133, 41–54.

Roberts, J.N., 1986. Comment about fractal sandstone pores. Phys. Rev. Lett. 56, 2111

Ross, P.J., Williams, J., Bristow, K.L., 1991. Equation for extending water-retention curves to dryness. Soil Sci. Soc. Am. J. 55, 923–927.

Senesi, N., 1996. Fractals in general soil science and in soil biology and biochemistry. In: Stotzky, G., Bollag, J-M. (Eds.), Soil Biochemistry, vol. 9. Dekker, New York, pp. 415–473.

Shepard, S.J., 1993. Using a fractal model to compute the hydraulic conductivity function. Soil Sci. Soc. Am. J. 57, 300–306.

Sokolowska, Z., 1989. On the role of energetic and geometric heterogeneity in sorption of water vapour by soils: application of a fractal approach. Geoderma 45, 251–265.

Toledo, P.G., Novy, R.A., Davis, H.T., Scriven, L.E., 1990. Hydraulic conductivity of porous media at low water content. Soil Sci. Soc. Am. J. 54, 673–679.

Turcotte, D.L., 1986. Fractal and fragmentation. J. Geophys. Res. 91, 1921–1926.

Turcotte, D.L., 1992. Fractal and Chaos in Geology and Geophysics. Cambridge University Press, Cambridge.

Tyler, S.W., Wheatcraft, S.W., 1989. Application of fractal mathematics to soil water retention estimation. Soil Sci. Soc. Am. J. 53, 987–996.

Tyler, S.W., Wheatcraft, S.W., 1990. Fractal processes in soil water retention. Water Resourc. Res. 26, 1047–1054.

Tyler, S.W., Wheatcraft, S.W., 1992a. Fractal scaling of soil particle-size distribution: analysis and limitations. Soil Sci. Soc. Am. J. 56, 362–369.

Tyler, S.W., Wheatcraft, S.W., 1992b. Reply. Water Resourc. Res. 28, 603–604.

Utomo, W.H., Dexter, A.R., 1981. Soil friability. J. Soil Sci. 32, 203–213.

Young, I.M., Crawford, J.W., 1991a. The fractal structure of soil aggregates: its measurement and interpretation. J. Soil Sci. 42, 187–192.

Young, I.M., Crawford, J.W., 1991b. The analysis of fracture profiles using fractal geometry. Aust. J. Soil Res. 30, 291–295.

Wittmus, H.D., Mazurak, A.P., 1958. Physical and chemical properties of soil aggregates in a Brunizem soil. Soil Sci. Soc. Am. Proc. 22, 1–5.

Wu, Q., Borkovec, M., Sticher, H., 1993. On particle-size distribution in soils. Soil Sci. Soc. Am. J. 57, 883–890.

Zeng, Y., Gantzer, C.J., Payton, R.L., Anderson, S.H., 1996. Fractal dimension and lacunarity of bulk density determined with X-ray computed tomography. Soil Sci. Soc. Am. J. 60, 1718–1724.